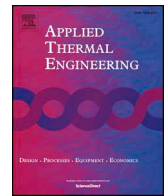




ELSEVIER

Contents lists available at ScienceDirect

Applied Thermal Engineering

journal homepage: www.elsevier.com/locate/apthermeng

Selection criteria of zeotropic mixtures for subcritical organic Rankine cycle based on thermodynamic and thermo-economic analysis

Zheng Miao^{a,b,*}, Zihang Li^a, Kai Zhang^a, Jinliang Xu^{a,b}, Yongpan Cheng^{a,b}

^a The Beijing Key Laboratory of Multiphase Flow and Heat Transfer for Low-Grade Energy, North China Electric Power University, 102206 Beijing, China

^b Key Laboratory of Power Station Energy Transfer Conversion and System (North China Electric Power University), Ministry of Education, 102206 Beijing, China

HIGHLIGHTS

- Thermodynamic and thermo-economic analyses are carried out.
- Selection criteria of zeotropic mixtures for the closed heat source are proposed.
- Heat source temperature drop is considered in the selection criteria.
- Selected mixtures show high thermodynamic and thermo-economic performance.

ARTICLE INFO

Keywords:

Organic Rankine cycle
Zeotropic mixtures
Thermo-economic analysis
Selection criteria
Levelized energy cost

ABSTRACT

The thermodynamic performance of an organic Rankine cycle can be improved effectively with zeotropic mixtures instead of pure fluid; however, it is quite challenging for the selection of zeotropic mixture to achieve the optimal thermodynamic and thermo-economic performance due to the lack of selection criteria. In this study, the thermodynamic and thermo-economic performance is evaluated in terms of overall exergy efficiency and the levelized energy cost respectively. The criteria for the selection of the optimal zeotropic mixture is revisited. It is found that our previously proposed criteria based on thermodynamic analysis for open heat source also holds for the thermo-economic analysis. Furthermore, the study for the effect of temperature drop on the selection of mixtures is carried out for the closed heat source. It is revealed that the heat source temperature drop can be divided into large, small, and transition regions, and the criteria for selection of optimal zeotropic mixture is proposed for each region. The thermo-economic analysis shows that the optimal thermodynamic and thermo-economic performance can be obtained simultaneously in the ORC system with the proposed selection criteria.

1. Introduction

To alleviate the serious global warming, energy crisis, and fossil fuel depletion, efficient energy conversion, and utilization technologies are urgently needed. The low-grade heat source provides a large amount of energy, such as geothermal energy and industrial waste heat, etc. In order to utilize low-grade energy, the organic Rankine cycle (ORC) is a promising technology to convert the heat to power [1,2]. To match the low-grade heat source, the organic fluid with low boiling temperature is adopted as working fluid instead of water steam [3–5], the working fluid can be pure substances or their mixture. The mixtures that have no zeotropic state existing in the two-phase region are referred to as the zeotropic mixtures. During the gas-liquid phase change process, the temperature keeps constant for pure fluid, while for zeotropic mixture

temperature glide exists, thus the temperatures in the heat source and working fluid can match well in the heat exchanger, resulting in reduced irreversible loss [6–8], hence the zeotropic mixture is attracting more and more attention from the researchers.

It has been widely proved that the ORC system with an azeotropic mixture performs better than that with pure working fluid [9–12]. So far there are plenty of substances for selection as the working fluid, and their mixtures are far more. Only a limited number of mixtures are studied, and the reasons are analyzed why they can improve the performance of ORC systems. However, the underlying mechanism is seldom revealed, the guidelines are also lacked to select the specified substances for the mixtures and their fractions at the given temperature of heat sources. The Edisonian approach is based on trial and error, which is not only computation-intensive but also inaccurate. Hence it is

* Corresponding author at: The Beijing Key Laboratory of Multiphase Flow and Heat Transfer for Low-Grade Energy, North China Electric Power University, 102206 Beijing, China.

E-mail address: miaozheng@ncepu.edu.cn (Z. Miao).

<https://doi.org/10.1016/j.applthermaleng.2020.115837>

Received 4 April 2020; Received in revised form 27 July 2020; Accepted 30 July 2020

Available online 07 August 2020

1359-4311/ © 2020 Elsevier Ltd. All rights reserved.

Nomenclature*List of symbols*

\dot{E}	exergy flow rate, kW
\dot{i}	exergy loss rate, kW
P	pressure, kPa
s	specific entropy, kJ/(kg·K)
\dot{W}	power, kW

Abbreviations

ORC organic Rankine cycle

Greek letters

η	efficiency
ξ	exergy loss coefficient

Subscripts and superscripts

bm	bare module
cf	cooling fluid
con	condensation or condenser
cri	critical state

eva	evaporator
exp	expander
hs	heat source
in	inlet
L	liquid
net	net output
h	specific enthalpy, kJ/kg
\dot{m}	mass flow rate, kg/s
\dot{Q}	heat transfer rate, kW
T	temperature, K
C	cost, \$
LEC	levelized energy cost
Δ	change or difference
out	outlet
p	pinch point
pump	pump
pre	precooling or preheating
sub	subcooling
sup	superheating
tot	total
V	vapor
wf	working fluid
*	optimal value

of great significance to find the criteria to select the optimal zeotropic mixtures according to their thermophysical properties instead of massive thermodynamic calculation. In our previous work [13] the criteria of zeotropic mixtures were proposed for subcritical ORC which is driven by the open heat source. 'Open' means there is no limitation on the outlet temperature of the heat source. If the outlet temperature is specified, it is called a closed heat source [14–16]. For example, if the ORC is used to recover heat from the flue gas of a coal-fired boiler, the heat source outlet temperature should be above 393.15 K to protect the heat exchanger from the acid dew point corrosion. Two correlations are adopted for mixture selection, which are $T_{hs} - T_{p_eva} = 1.182T_{cri}^* - 39.244$ (K) and $\Delta T_{wf_con}^* = \Delta T_{cf} - \Delta T_{sub}$, corresponding to the temperature match in the evaporator and condenser, respectively. Based on the temperature of the heat source/sink, the optimal critical temperature T_{cri}^* and condensation temperature glide $\Delta T_{wf_con}^*$ can be determined. These two temperatures are related to the thermophysical properties of the pure components and their concentrations in the mixture.

Herein, there are still two issues to be addressed: (1) how to select the optimal mixtures as working fluids for a closed heat source. (2) Whether the selected mixture by the thermodynamic criteria also has a

relatively higher thermo-economic performance. For the first issue, to the best knowledge of the authors, the selection criterion of the close heat source is still lacking. Most studies are focused on the performance comparison of the ORC system with mixture and pure fluids [17–19], in which inlet and outlet temperatures of heat sources are specified. Few studies analyzed the effect of the inlet temperature of the heat source on ORC performance [20,21]. Furthermore, the effect of the outlet temperature was neglected. Some mixtures are recommended in these works for a certain heat source. However, as mention above, the guidelines of how to select the mixtures are still lacked. Inspired by exergy analysis of the ORC [13,22] and the proposed selection criteria for pure working fluids [23,24], it is believed that the heat source temperature drop and the mixture critical temperature are the key factors for the mixture selection, which significantly affect the temperature match in the heat exchangers (evaporator and condenser).

For the second issue, the thermo-economic analysis should be carried out to evaluate thermo-economic performance. There have been extensive comparisons for the thermo-economic performance of the ORC system with zeotropic mixtures and pure fluids. Some studies showed that the ORC system with zeotropic mixtures performed better in the thermo-economic aspect [21,25–29] while other studies showed

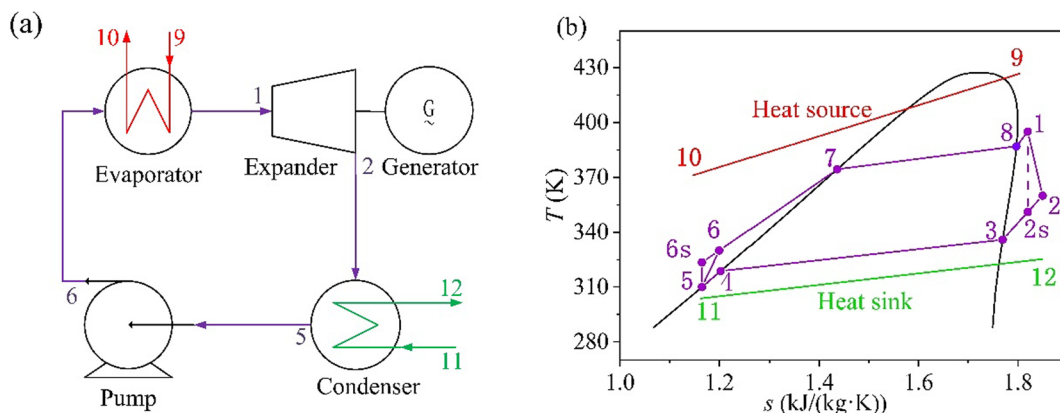


Fig. 1. (a) Schematic and (b) T - s diagram of a basic subcritical ORC.

the opposite conclusion [8,30,31]. Yang et al. [26] analyzed an ORC system using the mixture of R245fa/R236fa and found that the system with mixture has higher thermodynamic and economic performance than that with either pure-component of R245fa or R236fa. Heberle et al. [29] claimed that the overall thermo-economic performance with the mixture as a working fluid is better than that with the pure fluid in a geothermal ORC system. Le et al. [32] found that the ORC system with n-pentane showed the highest thermo-economic and thermodynamic performance, compared to the ORC using R245fa, and the mixture of n-pentane and R245fa. Oyewunmi et al. [33] found that mixtures result in more costs of the ORC system than the pure working fluid under the same net output power. The diverse results above is because the selected mixture may not match well with the heat source, leading to its poorer performance than the pure fluid, hence it is necessary to find the selection criteria for the optimal mixture according to both thermo-economic analysis and the thermodynamic analysis.

To address the issues above, in this study the thermodynamic and thermo-economic models on the ORC system are proposed Section 2 and validated first in Section 3.1. Then the thermo-economic performance of the ORC system with zeotropic mixtures selected through criteria for the open heat source is investigated in Section 3.2. Finally, the effect of the heat source temperature drop is studied, and the screening criteria are proposed for the closed heat source in Section 3.3 according to the thermodynamic and thermo-economic analysis.

2. Model description

2.1. System description

The schematic and T - s diagrams of a basic subcritical ORC are shown in Fig. 1. The system is composed of four fundamental equipment: evaporator, expander, condenser, and pump. The liquid working fluid is pumped to the evaporator and vaporized by the heat source, then the high-pressure vapor expands in the expander to generate mechanical work, finally, the exhaust vapor is condensed into liquid after releasing heat in the condenser.

2.2. Thermodynamic analysis

The thermodynamic analysis is established for the four main components, the heat source/sink as well as the system, based on the first and second laws of thermodynamics. The equations are listed in Table 1. The details can be found in our previous work [13]. The reference state is set at $T_0 = 293.15$ K and $P_0 = 1.01 \times 10^5$ Pa. The overall exergy efficiency is chosen as the thermodynamic index for the selection of mixtures as working fluid.

2.3. Thermo-economic analysis

The cost of every component in the ORC system is firstly calculated by the module costing technique [34], which is usually applied to assess the cost of chemical equipment. As the heat exchangers, expanders, and pumps are also common equipment involved in the chemical industry, many researchers adopted this technique to estimate the cost of the ORC system [21,28,29,35]. The bare module cost C_{bm} of equipment is calculated from [34]:

$$C_{bm} = C_p^0 F_{bm} \quad (1)$$

where C_p^0 is the procurement cost of the equipment in the base condition: working at the ambient pressure and made of common material, such as carbon steel. F_{bm} is the bare module factor considering the effect of operating pressure and material on the bare module cost of equipment. C_p^0 and F_{bm} are given as follows,

$$\log_{10} C_p^0 = K_1 + K_2 \log_{10}(Y) + K_3 [\log_{10}(Y)]^2 \quad (2)$$

$$F_{bm} = B_1 + B_2 F_m F_p \quad (3)$$

$$\log_{10} F_p = C_1 + C_2 \log_{10}(P) + C_3 [\log_{10}(P)]^2 \quad (4)$$

where the component capacity parameter Y refers to the heat transfer area, shaft power, and consumed power for the heat exchanger, expander, and pump, respectively. F_m is the material factor, and F_p is the pressure factor. P is the design pressure of the equipment. The coefficients $K_1 - K_3$, B_1 , B_2 , $C_1 - C_3$, F_m are given in Table 2.

The total cost of the ORC system depends mainly on the bare module cost of each component and can be calculated as:

$$C_{tot} = (C_{bm,eva} + C_{bm,exp} + C_{bm,con} + C_{bm,pump}) \frac{CEPCI_{2018}}{CEPCI_{2001}} \quad (5)$$

where $CEPCI$ is the Chemical Engineering Plant Cost Index which considers the variation of price with time. Based on the data reported in the literature [36–39], $CEPCI_{2001} = 397$ and $CEPCI_{2018} = 638.1$ were adopted. It is noted that the cost of working fluid is not taken into account in this work as many work have revealed that it attributes to less than 1% of the total cost [21,40–43].

The levelized energy cost (LEC) is chosen as the thermo-economic index, which is a synthetical index considering the thermodynamic and economic performance of the ORC system. It is given as follows:

$$LEC = (CRF \cdot C_{tot} + C_{om}) / (t_{op} \cdot \dot{W}_{net}) \quad (6)$$

where the capital recovery factor CRF and the operational and maintenance cost of the system C_{om} are calculated by

$$CRF = i(1+i)^{LT_{pl}} / [(1+i)^{LT_{pl}} - 1] \quad (7)$$

$$C_{om} = 1.5\% C_{tot} \quad (8)$$

The interest rate i , the equipment lifetime LT_{pl} , and the annual operation hour t_{op} are assumed to be moderate at 5%, 20 years, and 8000 h, respectively, according to reported data in the literature [29,35,37,38,44,45].

2.4. Heat exchanger model

The counter flow shell-tube heat exchanger is adopted as the evaporator and condenser. The logarithmic mean temperature difference (LMTD) [44] approach is used to calculate the heat transfer area. The heat source/sink fluid flows in the shell side. The heat source fluid is air and its mass flow rate is 10 kg/s. The heat sink fluid is water with an inlet temperature of 293.15 K and a temperature rise ΔT_{cf} of 10 K [38]. The Kern [46] correlation is used to calculate their Nusselt coefficients:

$$Nu = 0.36 Re^{0.55} Pr^{0.33} \quad (9)$$

Table 1

Basic equations of the thermodynamic analysis.

Components	Variables	Equations
Heat source	heat flux	$\dot{Q}_{hs} = \dot{m}_{wf}(h_1 - h_6) = \dot{m}_{hs}(h_9 - h_{10})$
	inlet exergy	$\dot{E}_{hs} = \dot{m}_{hs}(h_9 - h_0 - T_0(s_9 - s_0))$
evaporator	exergy loss	$\dot{I}_{eva} = T_0(\dot{m}_{wf}(s_1 - s_6) - \dot{m}_{hs}(s_9 - s_{10}))$
expander	shaft power	$\dot{W}_{exp} = \dot{m}_{wf}(h_1 - h_2) = \eta_{exp} \dot{m}_{wf}(h_1 - h_{2s})$
	exergy loss	$\dot{I}_{exp} = T_0 \dot{m}_{wf}(s_2 - s_{2s})$
pump	power consumed	$W_{pump} = \dot{m}_{wf}(h_6 - h_5) = \dot{m}_{wf}(h_{6s} - h_5) / \eta_{pump}$
	exergy loss	$\dot{I}_{pump} = T_0 \dot{m}_{wf}(s_6 - s_{6s})$
condenser system	exergy loss	$\dot{I}_{con} = T_0(\dot{m}_{cf}(s_{12} - s_{11}) - \dot{m}_{wf}(s_2 - s_5))$
	thermal efficiency	$\eta_I = \dot{W}_{net} / \dot{Q}_{hs} = (\dot{W}_{exp} - \dot{W}_{pump}) / \dot{Q}_{hs}$
	coefficient of exergy loss	$\xi_i = \dot{I}_i / \dot{E}_{hs}^{(i)}$
	overall exergy efficiency	$\eta_{II} = \dot{W}_{net} / \dot{E}_{hs} = 1 - \sum \xi_i^{(i)}$

^a I denotes the different components in the ORC cycle, including the heat source/sink, the evaporator, condenser, expander, and pump.

Table 2
The costing coefficient of the components of the ORC system [34].

Coefficient	Pump	Evaporator	Condenser	Expander
K_1	3.3892	4.3247	4.3247	3.514
K_2	0.0536	-0.303	-0.303	0.598
K_3	0.1538	0.1634	0.1634	0
C_1	-0.3935	0.03881	0.03881	/
C_2	0.3957	-0.11272	-0.11272	/
C_3	-0.00226	0.08183	0.08183	/
B_1	1.89	1.63	1.63	/
B_2	1.35	1.66	1.66	/
F_m	1.55	1.35	1.35	/
F_{bm}	/	/	/	1.5

Pure or mixture working fluid flows in the tube side. The Gnielinski correlation [47] is used for the single-phase convective heat transfer:

$$Nu = \frac{(f/8)(Re - 1000)Pr}{1 + 12.7(f/8)^{0.5}(Pr^{2/3} - 1)} \quad (10)$$

$$f = [0.790 \ln(Re) - 1.64]^{-2} \quad (11)$$

The boiling heat transfer coefficient α_{TP} is obtained from the Gungor-Winterton correlation [48] with the correction factors F_c for mixture working fluid proposed by Thome [49]:

$$\alpha_{TP} = E\alpha_L \quad (12)$$

$$E = 1 + 3000(BoFc)^{0.86} + 1.12\left(\frac{x}{1-x}\right)^{0.75}\left(\frac{\rho_L}{\rho_V}\right)^{0.41} \quad (13)$$

$$\alpha_L = 0.023Re_L^{0.8}Pr_L^{0.4}\frac{k_L}{d_i} \quad (14)$$

$$F_c = \left\{ 1 + \left(\frac{\alpha_{id}}{q}\right)\Delta T_{evp} \left[1 - \exp\left(\frac{-qB_0}{\rho_L\Delta H_{vap}\beta_L}\right) \right] \right\}^{-1} \quad (15)$$

where F_c is equal to 1 for the pure working fluid. α_{id} is α_L in Eq. (14) but with the mixture's physical properties. ΔT_{evp} is the temperature glide during boiling; B_0 is the ratio factor, and β_L is the mass transfer coefficient.

The condensation heat transfer coefficient of the pure working fluid is calculated from the Shah correlation [50]:

$$\alpha_{TP} = \begin{cases} \alpha_1, J_V \geq 0.98(Z + 0.263)^{-0.62} \\ \alpha_1 + \alpha_{Nu}, J_V \geq 0.98(Z + 0.263)^{-0.62} \end{cases} \quad (16)$$

$$\alpha_1 = \alpha_L \left(1 + \frac{3.8}{Z^{0.95}} \right) \left(\frac{\mu_L}{14\mu_V} \right)^{(0.0058+0.557Pr)} \quad (17)$$

$$\alpha_{Nu} = 1.32Re_L^{(-1/3)} \left[\frac{\rho_L(\rho_L - \rho_V)gk_L^3}{\mu_L^2} \right]^{1/3} \quad (18)$$

where the expressions of parameter J_V and Z can be found in the literature [50]. For the condensation of a mixture, the correction approach proposed by Bell and Ghaly [51] for Shah correlation is applied:

$$\frac{1}{\alpha_{mix}} = \frac{1}{\alpha_{mono}} + \frac{Y_V}{\alpha_V} \quad (19)$$

$$Y_V = xC_{pv} \frac{\Delta T_{con}}{\Delta H_{vap}} \quad (20)$$

where α_{mono} is α_{TP} in Eq. (16) but with the mixture's physical properties. C_{pv} is the specific heat capacity of the vapor phase and ΔT_{con} is the condensation temperature glide.

2.5. Calculation method and conditions

Fig. 2 shows the computational flow chart. For a specified heat source inlet temperature, the heat source outlet temperature was

assumed initially and adjusted iteratively to achieve the highest exergy efficiency under the constraint of the pinch temperature difference. The evaporation and condensation pressures are also updated iteratively to make the minimum temperature difference in the heat exchanger approach the given pinch temperature difference. The liquid, two-phase, and vapor sections shown in Fig. 1 are further discretized into hundreds of sub-sections to calculate the temperature difference accurately based on the energy conservation equation. The working fluid properties are calculated from the Refprop 9.0 database. The main operation parameters are shown in Table 3.

Assumptions used in the thermodynamic analysis are presented as follows:

- (1) The working fluid at the outlet of the expander is saturated or superheated to ensure no liquid entrainment in the expander.
- (2) The pressure drop and heat loss in the evaporator and condenser are neglected.
- (3) The isentropic efficiencies of the expander and pump are assumed as 0.8 [52,53] and 0.75 [52,54].
- (4) The maximum evaporation pressure is restricted below 90% of the working fluid critical pressure to ensure the safe operation of the ORC system.

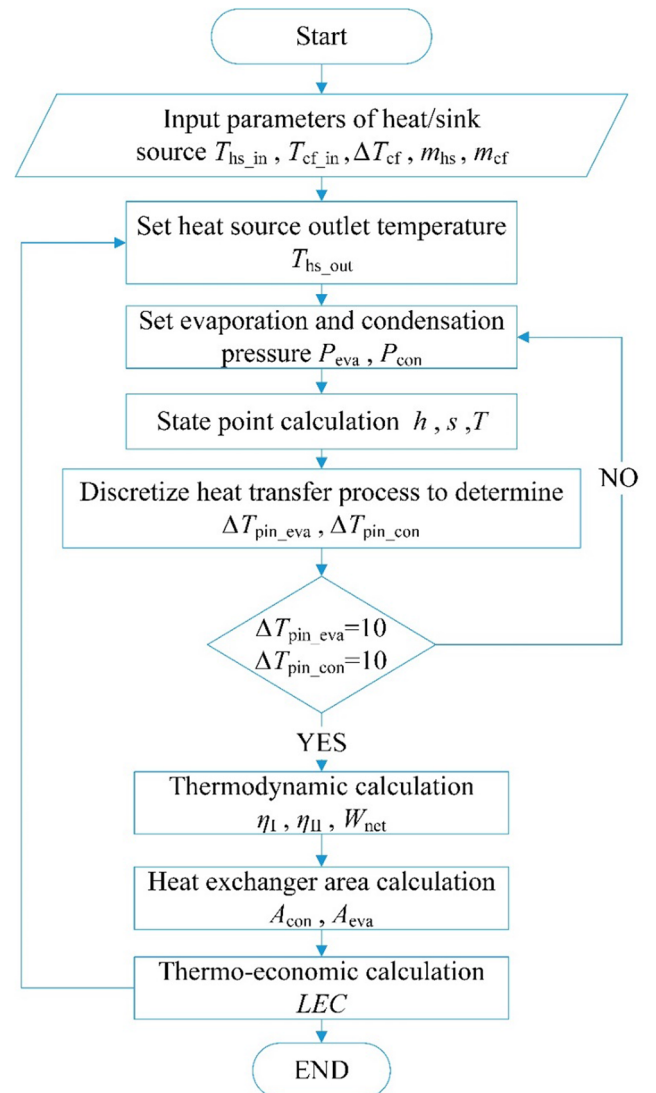


Fig. 2. Computational flow chart.

Table 3
Calculation conditions of the model.

Parameters	Symbol	Value	Reference
The pinch temperature difference in the evaporator	$T_{p,eva}$	10 K	[23,55,56]
The pinch temperature difference in the condenser	$T_{p,con}$	10 K	[22,57]
Subcooling degree in the condenser output	ΔT_{sub}	0 K, 5 K	
Heat source inlet temperature	$T_{hs,in}$	393.15 K-623.15 K	

3. Results and discussion

3.1. Model validation

The present model was validated with the results of Chys et al. [58] who studied the ORCs with R245fa, R365mfc, and their mixtures. Use the same heat source/sink parameters as those in literature [58], the results are summarized in Table 4. It is seen that the results of the present model agree well with the reported data, indicating the reliability of the simulation in the present work.

3.2. Thermo-economic analysis of the ORC with an open heat source

In this section, the thermo-economic performance of the ORC using mixtures selected by the thermodynamic criteria for the open heat source in our former work [13] is evaluated. Detailed information on the mixtures can be found in the literature [13]. The criteria consist of two correlations: $T_{hs} - T_{p,eva} = 1.182T_{cri}^* - 39.244$ (K) and $\Delta T_{wf,con}^* = \Delta T_{cf} - \Delta T_{sub}$. The first correlation was used to calculate the optimal mixture critical temperature T_{cri}^* . It was proved that the optimization of the temperature match in the evaporator improve the cycle performance more significantly than that in the condenser. After forming a series of mixtures all with T_{cri}^* , the mixtures with a condensation temperature glide near the optimal temperature glide $\Delta T_{wf,con}^*$ were selected. Due to the discontinuous variation of the condensation temperature glide, a temperature range ± 2 K is added to $\Delta T_{wf,con}^*$.

3.2.1. Bare module cost of the main components and ORC system

The heat source inlet temperature $T_{hs,in}$ of 423.15 K, 503.15 K, and 583.15 K are considered to make a comparison study. The bare module cost of the evaporator, condenser, and expander as well as the total cost of the ORC system for mixture with different T_{cri} are shown in Fig. 3. The dashed lines represent T_{cri}^* predicted by the first correlation, which is 382.7 K, 450.4 K, and 518.1 K, respectively.

Generally speaking, $C_{bm,eva}$, $C_{bm,con}$, and $C_{bm,exp}$ become higher with the increase in $T_{hs,in}$. It indicates an increase in the output power of the ORC system. The highest $C_{bm,eva}$, and $C_{bm,exp}$ appear near the dashed lines, indicating that more heat transfer area and expander power are needed for the mixture with T_{cri}^* . It is because the temperature difference between the heat source and the working fluid is reduced while the working fluid with T_{cri}^* providing the optimal temperature match in the evaporator and condenser. Besides, the change of $C_{bm,con}$ is quite small when T_{cri} is lower than 520 K. Thus, the variation of C_{tot} is determined by those of $C_{bm,eva}$, and $C_{bm,exp}$. The relatively high C_{tot} at T_{cri}^* implies that the optimal mixtures from a thermodynamic point of view

Table 4
Validation of the present model [58].

	Composition ratio (mole)		P_{eva} (kPa)	P_{con} (kPa)	m_{wf} (kg/s)	P_{pump} (kW)	P_{gen} (kW)	η_{II} (%)
R245fa	1	M. Chys	2030	290	4.47	-7.5	100.3	9.61
		Present work	2026	287	4.47	-7.5	100.3	9.62
R365mfc	1	M. Chys	940	120	4.25	-3.6	104.1	10.40
		Present work	943	118	4.25	-3.6	104.0	10.41
R245fa- R365mfc	0.30-0.70	M. Chys	1310	150	4.28	-5.0	109.5	10.82
		Present work	1272	148	4.26	-4.9	108.3	10.75

require higher investment cost. For T_{cri} higher than 520 K, $C_{bm,con}$, and C_{tot} increase rapidly with T_{cri} . It reflects that the thermodynamic and economic performance will be deteriorated if the mixture working fluid has too high T_{cri} .

3.2.2. Thermo-economic performance considering the optimal critical temperature

Integrating the thermodynamic and thermo-economic analysis, the overall exergy efficiency η_{II} and levelized energy cost LEC under different $T_{hs,in}$ are shown in Fig. 4. It is seen that the LEC exhibits a very gentle variation trend with the increase in T_{cri} , first reduces and then increases. The higher overall exergy efficiency η_{II} near T_{cri}^* always corresponds to a smaller LEC , which indicates the improvement of thermodynamic performance through optimizing the temperature match is more significant than the deterioration of economic performance caused by the increasing heat transfer area. In addition, it is seen that the optimal η_{II} goes higher with the increase in the $T_{hs,in}$ while the LEC becomes lower. Thus, the thermodynamic and thermo-economic performance of the ORC system could be optimized by increasing the $T_{hs,in}$. This trend is similar to the results in the literature [21].

3.2.3. Thermo-economic performance considering the optimal condensation temperature glide

Lots of mixtures with the same critical temperature (T_{cri}^*) can be obtained by adjusting the concentration of pure substances. However, these mixtures have different condensation temperature glide. Fig. 5 illustrates the η_{II} and LEC of the ORC system using mixtures all with $T_{cri}^* = 382.7$ K. Two subcooling degrees ΔT_{sub} of 0 K and 5 K are employed to investigate its influence on the optimal region of condensation temperature glide. As the temperature rise of cooling water ΔT_{cf} is 10 K, the $\Delta T_{wf,con}^*$ is calculated to be 10 K and 5 K, respectively, based on the correlation [13] $\Delta T_{wf,con}^* = \Delta T_{cf} - \Delta T_{sub}$. Thus, the optimal region shown in Fig. 5 is 8-12 K for $\Delta T_{sub} = 0$ K, and 3-7 K for $\Delta T_{sub} = 5$ K considering a temperature range of ± 2 K. It is seen that mixtures in the optimal region exhibit the higher η_{II} and lower LEC , indicating that the selection criteria can predict suitable zeotropic mixtures effectively both from the thermodynamic and thermo-economic points of view.

3.2.4. The optimal outlet temperature of the open heat source

For a given $T_{hs,in}$ and $T_{cf,in}$, the proper mixture can be screened out, then the heat source outlet temperature $T_{hs,out}$ is obtained from the thermodynamic analysis of the cycle. The $T_{hs,out}$ corresponds to the maximum η_{II} of the cycle is defined as the optimal outlet temperatures of the open heat source $T_{hs,out}^*$. We summarized the $T_{hs,out}^*$ under

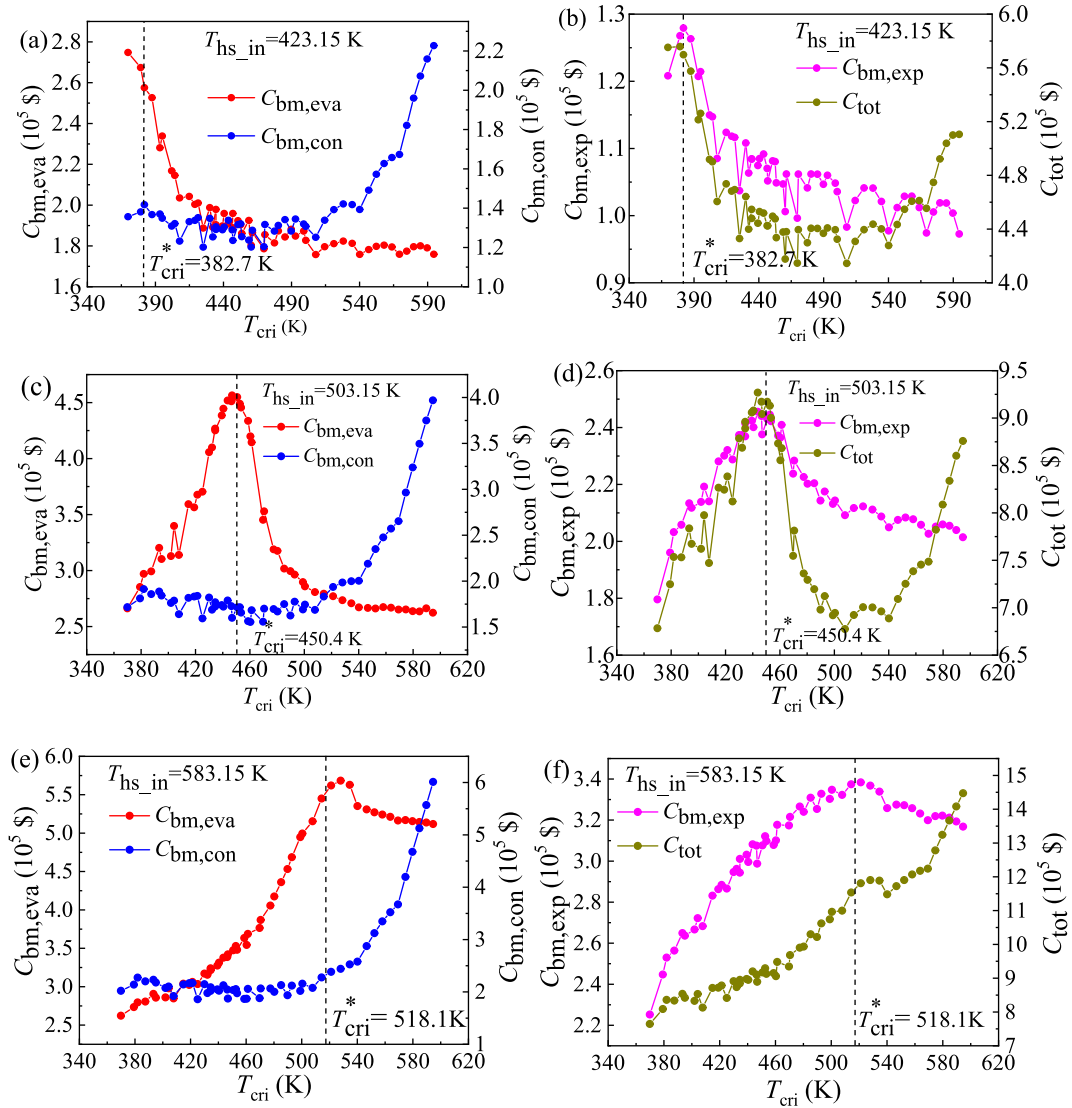


Fig. 3. Equipment cost and total cost of system under heat source inlet temperature of (a–b) 423.15 K, (c–d) 503.15 K, and (e–f) 583.15 K.

different $T_{hs,in}$ in Fig. 6. It is seen that $T_{hs,out}^*$ is distributed in a narrow temperature range of 20 K (from 313 K to 333 K) while the $T_{hs,in}$ varies significantly from 413.15 K to 623.15 K. In the present work, 313 K is the lower limit of $T_{hs,out}^*$ as it is the sum of the cooling water inlet temperature $T_{cf,in}$, the pinch temperature difference in the condenser $T_{p,con}$ and the pinch temperature difference in the evaporator $T_{p,eva}$, shown in Fig. 6(b). If the given outlet temperature of a closed heat source falls in this range, the closed heat source can be treated as an open heat source. Thus, the selection criteria of zeotropic mixtures proposed in our former work [13] are still applicable. If the outlet temperature of the closed heat source is higher than the 20 K range, further analysis is implemented in the next section.

3.3. Selection criteria of zeotropic mixture for the ORC with a closed heat source

In this section, we also use the η_{II} and LEC as the thermodynamic index and thermo-economic index to select mixture working fluids.

3.3.1. Effect of heat source temperature drop on system thermodynamic performance

Fig. 7 shows the variation of η_{II} with T_{cri} under different ΔT_{hs} . When ΔT_{hs} is large (70 K, 80 K), η_{II} decreases monotonically with T_{cri} . When

ΔT_{hs} is small (20 K, 30 K), η_{II} increases rapidly first and then decreases gently as T_{cri} increases. This trend agrees with results in the literature [24] which studied the effect of critical temperature on the selection of pure working fluid. The divergent trends indicate that the mixtures with relatively lower T_{cri} are preferred to the large ΔT_{hs} while the mixtures with higher T_{cri} can provide higher thermodynamic performance at the small ΔT_{hs} .

Fig. 8 shows the coefficients of exergy loss in main equipment and explains why η_{II} exhibits divergent trends in Fig. 7. It is clear that the variation of the sum $\xi_{eva} + \xi_{con} + \xi_{exp}$ is determined by ξ_{eva} . ξ_{con} increases gently with T_{cri} at both the large and small ΔT_{hs} while ξ_{exp} shows the contrary trend. They offset each other and highlight the effect of ξ_{eva} .

ξ_{eva} is directly related to the temperature match between the heat source and working fluid in the evaporator. Fig. 9 shows the T - s diagrams of mixtures different T_{cri} with under large and small ΔT_{hs} . It is seen that the constant-pressure line (green lines) in the evaporator has a much steeper slope in the preheating region than the two-phase liquid-vapor region. As a result, the heat source with a large ΔT_{hs} can thermally match well with the working fluid at the preheating region but poor at the two-phase liquid-vapor region, shown in Fig. 9(a) and (b). Thus, the irreversible loss is mainly caused by the heat transfer at the two-phase liquid-vapor region. In this situation, it is expected to have a

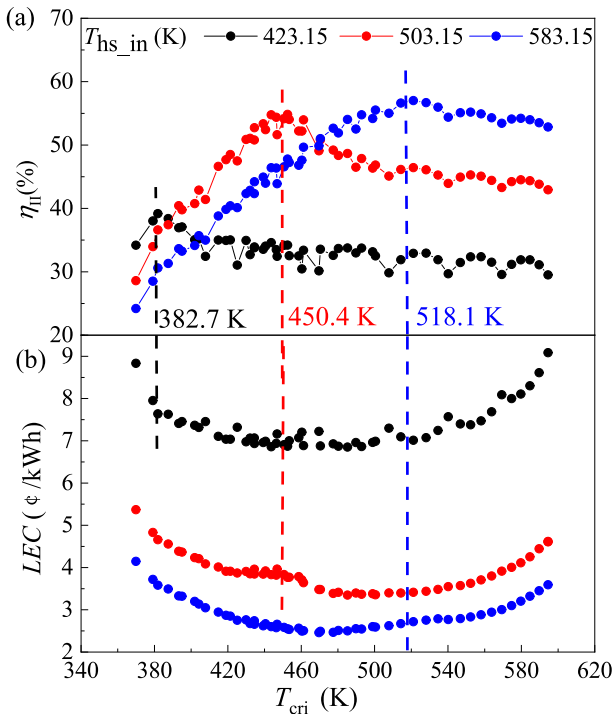


Fig. 4. The variation of (a) η_{II} and (b) LEC with the T_{cri} of working fluid under different $T_{hs,in}$.

longer constant-pressure line in the preheating region. Consequently, the mixture with a lower T_{cri} is preferable. Fig. 9(c) and (d) show the same logic. the mixture with a relatively higher T_{cri} is suitable for the heat source with a smaller ΔT_{hs} .

3.3.2. Division of heat source temperature drop and determination of the preferred mixtures

Analysis in Section 3.3.1 indicates that ΔT_{hs} is a sensitive parameter that should be considered in the selection of working fluid. It is expected to study the transition between the two trends shown in Fig. 7. Further analysis of η_{II} under different $T_{hs,in}$ and ΔT_{hs} was carried out to

explore the principles of how to classify the temperature drop into different regions and its effect on the selection of working fluid. The results are summarized in Figs. 10–11.

Fig. 10 shows the division of ΔT_{hs} . Three regions are marked out by two lines obtained by the linear fitting. The red solid line is the upper bound corresponding to $\Delta T_{hs}^{upper} = 0.709T_{hs,in} - 243.07$ (K) and ΔT_{hs} over this line can be treated as a large temperature drop. The blue solid line is the lower bound corresponding to $\Delta T_{hs}^{lower} = 0.56T_{hs,in} - 196.297$ (K). ΔT_{hs} below the line is treated as a small temperature drop.

Temperature drop regions in Fig. 10 is directly related to the variation of η_{II} with T_{cri} . Accordingly, the principles of selecting mixture working fluids can be achieved. Fig. 11 shows the influence of the temperature drop on the working fluid selection. The heat sources inlet temperature of 423.15 K and 448.15 K are selected for the present analysis. The upper and lower bound temperature drop is calculated as 56.9 K and 40.7 K for the inlet temperature of 423.15 K while 74.7 K and 54.7 K for the inlet temperature of 448.15 K. It is seen that η_{II} decreases monotonously with T_{cri} in the large temperature drop region (red points). The relatively high exergy efficiency can be achieved when the mixture critical temperature is below $T_{hs,in} - T_{p,eva} + 30$ K, represented by the purple dashed line in Fig. 11. Regarding the small temperature drop region (blue points), the η_{II} increases rapidly at first and then decreases much gentler with the increasing T_{cri} . The maximum η_{II} appears near the blue line which represents the temperature of $T_{hs,in} - T_{p,eva} + 70$ K. The mixtures with the critical temperature higher than and close to $T_{hs,in} - T_{p,eva} + 70$ K are recommended. When ΔT_{hs} locates in the transition region (black points), the mixtures with the critical temperature in the range of $T_{hs,in} - T_{p,eva} + 30$ K to $T_{hs,in} - T_{p,eva} + 70$ K can provide relatively high η_{II} .

3.3.3. Thermo-economic analysis of the ORC with a closed heat source

Fig. 12 depicts the variation of the thermodynamic index η_{II} and the thermo-economic index LEC with the increase in T_{cri} . The purple line represents the temperature of $T_{hs,in} - T_{p,eva} + 30$ K and the blue line is $T_{hs,in} - T_{p,eva} + 70$ K. When ΔT_{hs} is in the large temperature region, shown in Fig. 12(a), the mixtures locate at the left of the purple line are recommended. It is seen that η_{II} is relatively higher and LEC is lower in this region. Thus, the thermodynamic and the thermo-economic indexes can be satisfied at the same time. For the small ΔT_{hs} shown in Fig. 12(b), the working fluid at the right side of the blue line is preferable based on the analysis in the section above. It is seen that thermodynamic and

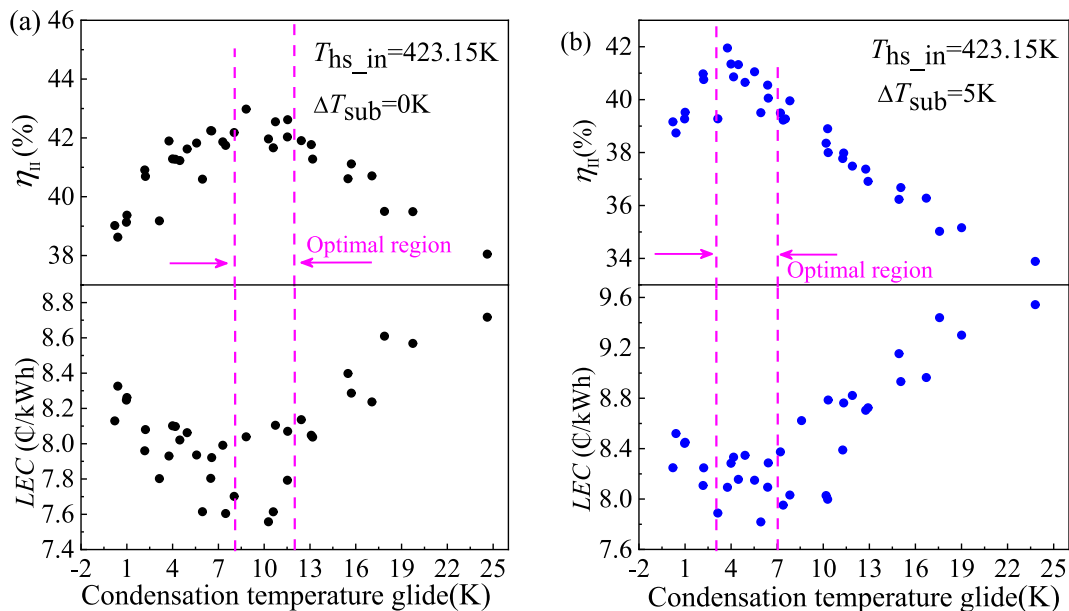


Fig. 5. The variation of η_{II} and LEC with condensation temperature glide for (a) $\Delta T_{sub} = 0$ K and (b) $\Delta T_{sub} = 5$ K.

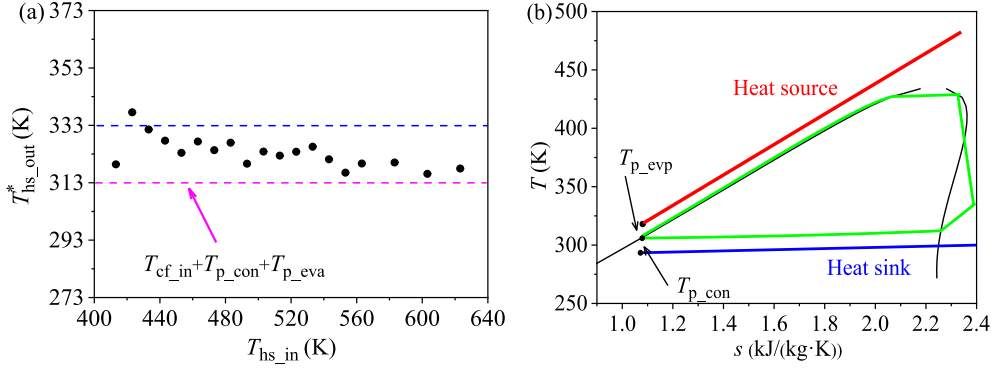


Fig. 6. Optimal heat source outlet temperature corresponding to the selected mixtures under different $T_{hs,in}$.

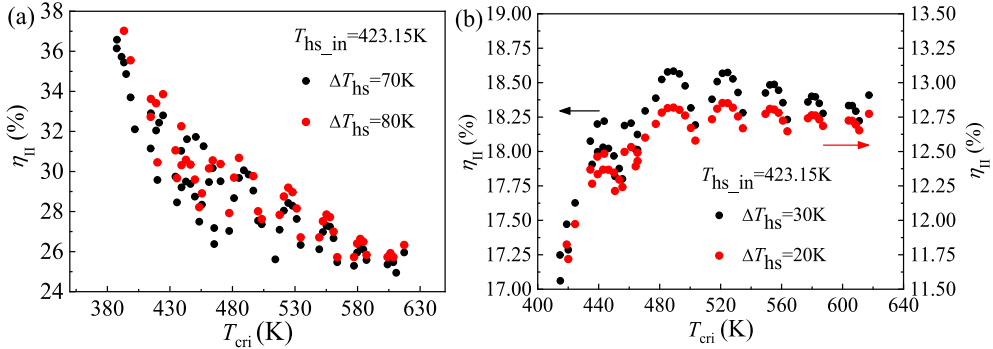


Fig. 7. Overall exergy efficiency of ORC using mixtures at the (a) large and (b) small heat source temperature drop.

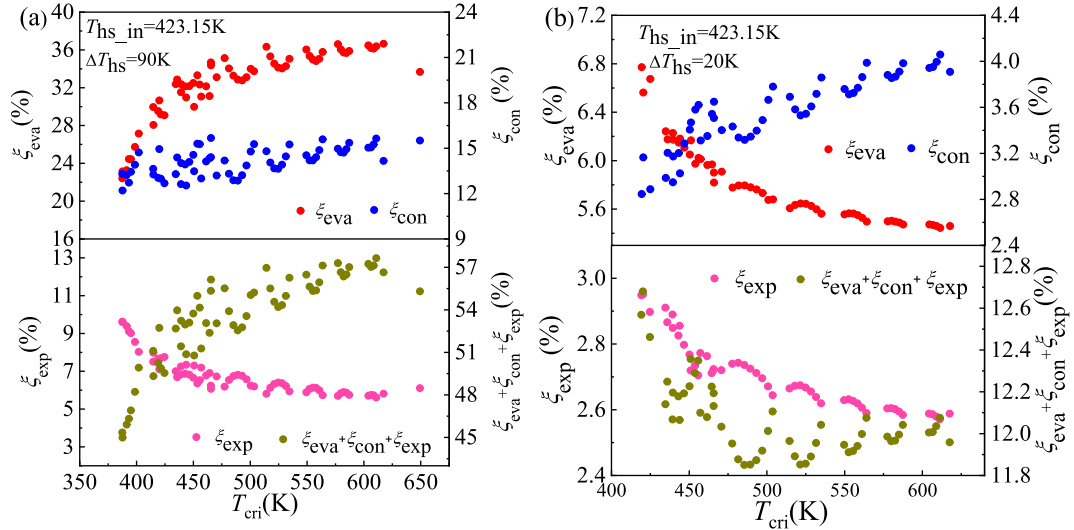


Fig. 8. Coefficient of the exergy loss in main components under (a) large and (b) small heat source temperature drops.

thermo-economic indexes can also be satisfied. It is noted that T_{cri} should be higher and close to $T_{hs,in} - T_{p,eva} + 70$ K because the LEC will increase significantly when T_{cri} is far from the blue line.

The local fluctuation of η_{II} is related to the different condensation temperature glide as these points corresponding to the mixtures with the same components but different concentrations. As the temperature match in the condenser is sensitive to the mixture's condensation temperature glide but not the type of heat source (open or closed), the correlation $\Delta T_{wf_con}^* = \Delta T_{cf} - \Delta T_{sub}$, proposed in our former work [13] for the open heat source is also applicable for the closed heat source to screen out the mixture with proper condensation temperature glide among these fluctuation points.

3.3.4. Selection criteria of mixtures for the closed heat source

Accordingly, the selection criteria of mixtures for the closed heat source can be proposed as follows:

- (1) *Check the heat source outlet temperature.* If $T_{hs,out}$ falls in the range of $T_{cf,in} + T_{p,eva} + T_{p,con}$ to $T_{cf,in} + T_{p,eva} + T_{p,con} + 20$ K, the closed heat source can be treated as an open heat source. Thus, the selection criteria of zeotropic mixtures proposed in our former work [13] are still applicable.
- (2) *Determine the type of temperature drop.* If the heat source cannot be treated as an open heat source, calculate ΔT_{hs} . Then the corresponding temperature drop region can be determined according to the upper and lower bound correlations.

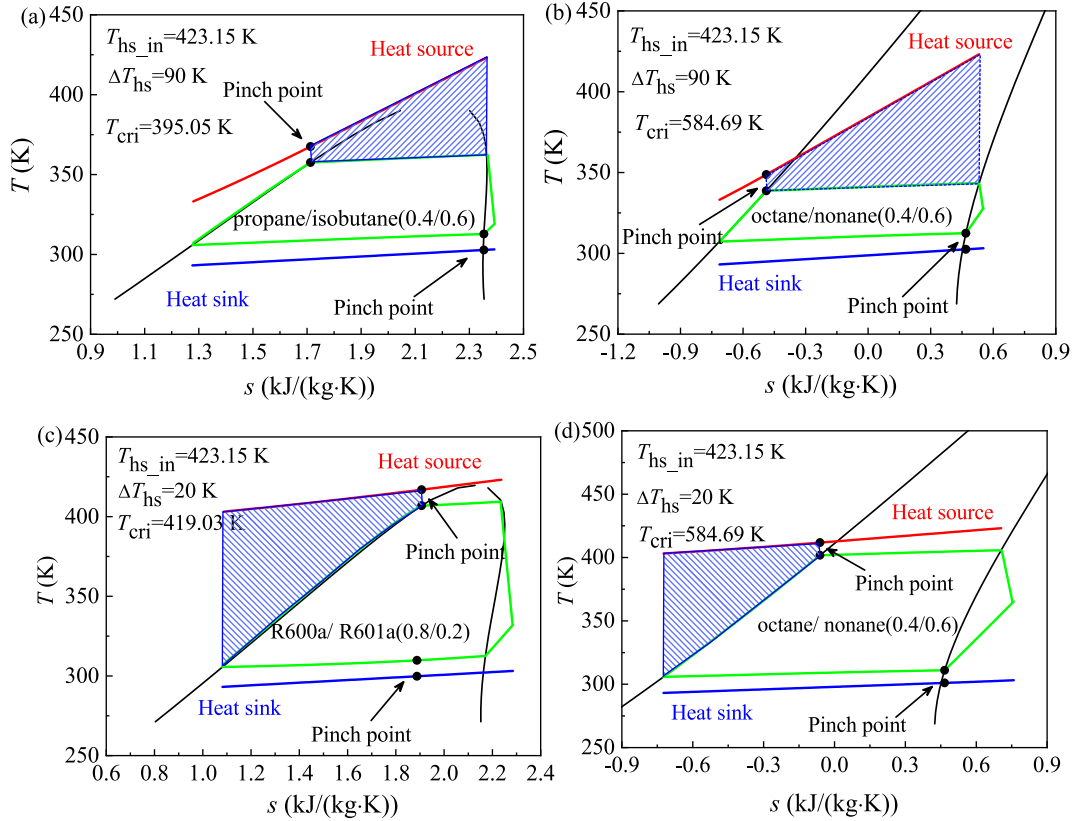


Fig. 9. Temperature match between low/high T_{cri} working fluid with heat source under (a–b) large and (c–d) small temperature drop.

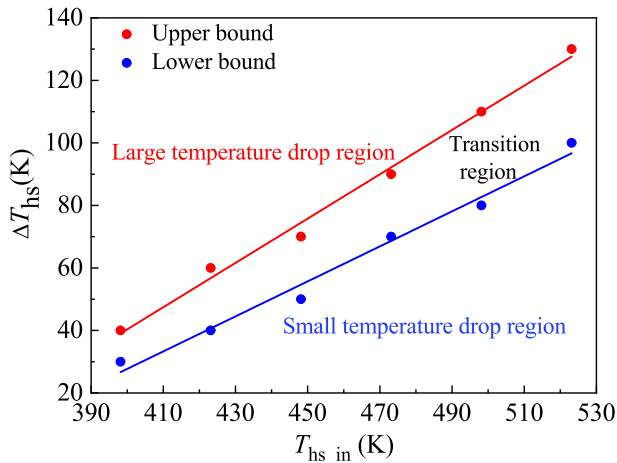


Fig.10. Determination of temperature drop region of heat source.

- (3) *Recommend the suitable mixture components.* Based on the temperature drop region determined in the second step, the optimal mixtures should have the critical temperature of $T_{cri} \leq (T_{hs,in} - T_{p,eva} + 30 \text{ K})$ for the large ΔT_{hs} ; $T_{cri} \geq (T_{hs,in} - T_{p,eva} + 70 \text{ K})$ for the small ΔT_{hs} , and $(T_{hs,in} - T_{p,eva} + 30 \text{ K}) \leq T_{cri} \leq (T_{hs,in} - T_{p,eva} + 70 \text{ K})$ for the transition region.
- (4) *Recommend the proper mixture concentration.* The proper mixture concentration can be determined according to the correlation $\Delta T_{wf,con}^* = \Delta T_{cf} - \Delta T_{sub} \pm \alpha$. $\alpha = 2\text{K}$ is recommended.

It is worth emphasizing that the proposed selection criteria for the closed heat source are more effective when $T_{hs,in}$ is below 473.15 K. For $T_{hs,in}$ above 473.15 K, ξ_{con} fluctuates in a large range due to the dry and

wet properties of the mixtures. In this situation, these selection criteria become less effective. The proposed selection criteria for open and closed heat sources are based on the thermodynamic and thermo-economic analysis, thus further consideration of the toxicity, flammability, and environment-friendliness of the mixtures is necessary. Furthermore, the present work is for the sub-critical ORC, the study on the selection criteria of mixtures for the super-critical ORC is underway.

4. Conclusions

In the present work, the thermodynamic and thermo-economic analysis of the ORC using zeotropic mixture working fluids were carried out. Thermo-economic performance of the ORC with mixtures selected from the thermodynamic criteria for open heat source was evaluated. The selection criteria for the closed heat source was proposed. The main findings are presented as follows:

- (1) The zeotropic mixtures selected by the proposed criteria can realize the high overall exergy efficiency and low leveled energy cost simultaneously as the improvement of thermodynamic performance through optimizing the temperature match is more significant than the increased investment cost due to the increased heat transfer area.
- (2) The closed heat source can be treated as an open heat source if its outlet temperature falls in the range of $T_{cf,in} + T_{p,eva} + T_{p,con}$ to $T_{cf,in} + T_{p,eva} + T_{p,con} + 20 \text{ K}$. The selection criteria of zeotropic mixtures for the open heat source are also applicable for the closed heat source in this situation.
- (3) For a closed heat source, the heat source temperature drop has a significant effect on the selection of working fluid. It can be divided into large, small, and transition regions by correlations of $\Delta T_{hs}^{upper} = 0.709T_{hs,in} - 243.07 \text{ (K)}$ and $\Delta T_{hs}^{lower} = 0.56T_{hs,in} - 196.297 \text{ (K)}$.
- (4) The selection criteria for the closed heat source are $T_{cri} \leq (T_{hs,in} -$

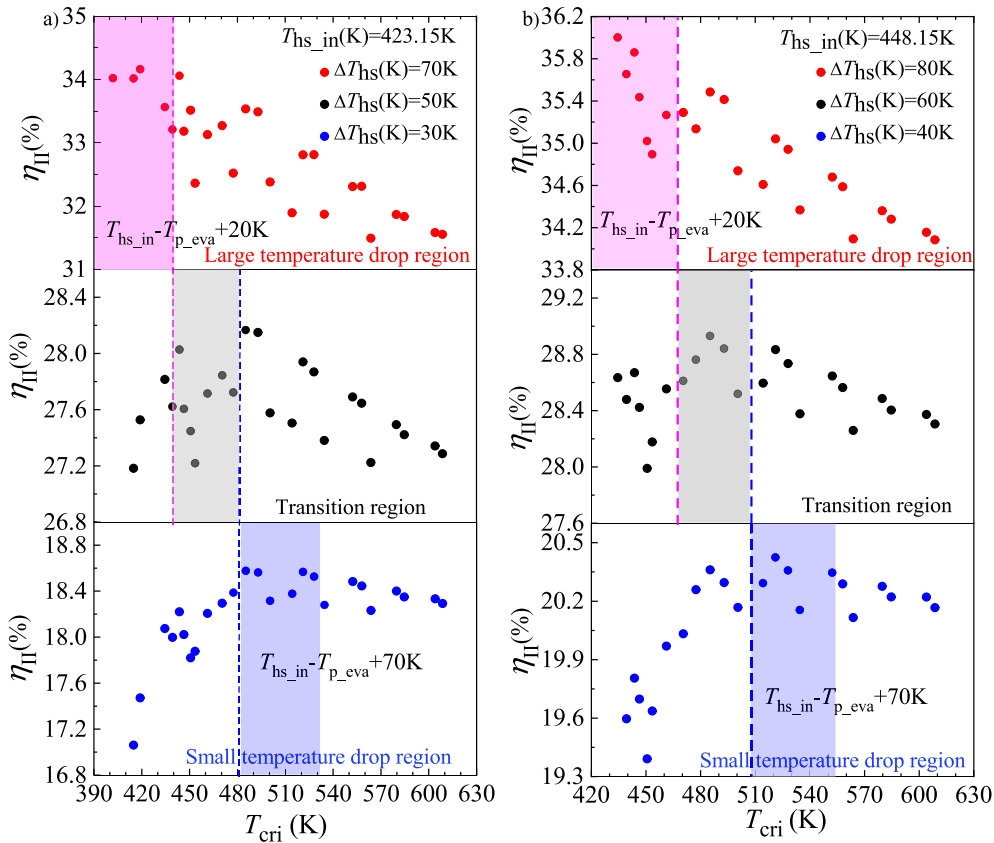


Fig. 11. The overall exergy efficiency of the ORC system in different temperature drop region under different heat source inlet temperature.

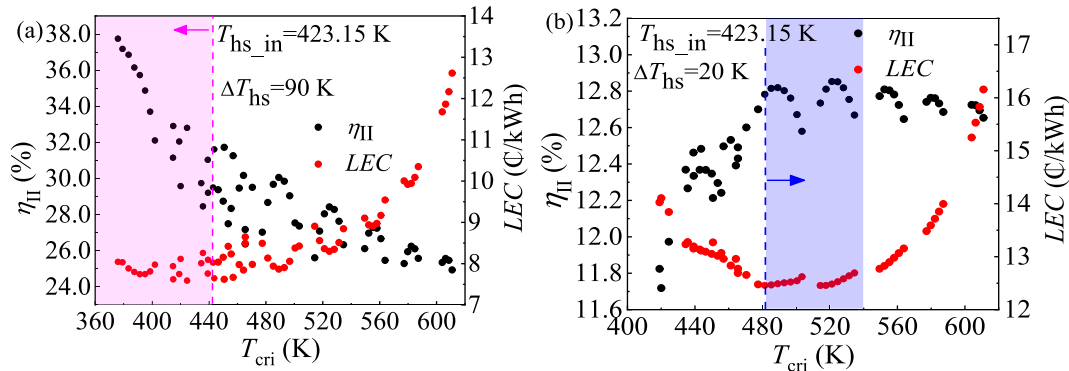


Fig. 12. Overall exergy efficiency and LEC for (a) large and (b) small heat source temperature drops.

$T_{p,eva} + 30 \text{ K}$) for the large temperature drop region; $(T_{hs,in} - T_{p,eva} + 30 \text{ K}) \leq T_{cri} \leq (T_{hs,in} - T_{p,eva} + 70 \text{ K})$ for the transition region and $T_{cri} \geq (T_{hs,in} - T_{p,eva} + 70 \text{ K})$ for the small temperature drop region. The correlation $\Delta T_{wf,con}^* = \Delta T_{cf} - \Delta T_{sub}$ is adopted to determine the proper mixture concentration for both the open and closed heat sources.

Declaration of Competing Interest

The authors declare that they have no known competing financial interests or personal relationships that could have appeared to influence the work reported in this paper.

Acknowledgment

The authors highly appreciate the support of the National Natural Science Foundation of China (No. 51776064) and the Fundamental

Research Funds for the Central Universities (No. 2020DF002, No. 2018MS018).

Appendix A. Supplementary material

Supplementary data to this article can be found online at <https://doi.org/10.1016/j.applthermaleng.2020.115837>.

References

- [1] T.C. Hung, T.Y. Shai, S.K. Wang, A review of organic rankine cycles (ORCs) for the recovery of low-grade waste heat, *Energy* 22 (1997) 661–667.
- [2] D. Di Battista, R. Cipollone, C. Villante, C. Fornari, M. Mauriello, The potential of mixtures of pure fluids in ORC-based power units fed by exhaust gases in internal combustion engines, *Energy Procedia* 101 (2016) 1264–1271.
- [3] Z. Miao, J. Xu, K. Zhang, Experimental and modeling investigation of an organic Rankine cycle system based on the scroll expander, *Energy* 134 (2017) 35–49.
- [4] T.C. Hung, Waste heat recovery of organic Rankine cycle using dry fluids, *Energy Convers. Manage.* 42 (2001) 539–553.

- [5] T. Eller, F. Heberle, Thermodynamic and economic analysis of geothermal combined heat and power based on a double-stage Organic Rankine Cycle, in: 5th Int. Semin. ORC Power Syst., Athens, Greece, 2019.
- [6] A. Modi, F. Haglind, A review of recent research on the use of zeotropic mixtures in power generation systems, *Energy Convers. Manage.* 138 (2017) 603–626.
- [7] L. Zhao, J. Bao, Thermodynamic analysis of organic Rankine cycle using zeotropic mixtures, *Appl. Energy*. 130 (2014) 748–756.
- [8] G. Bamorovat Abadi, K.C. Kim, Investigation of organic Rankine cycles with zeotropic mixtures as a working fluid: Advantages and issues, *Renew. Sustain. Energy Rev.* 73 (2017) 1000–1013.
- [9] J. Lu, J. Zhang, S. Chen, Y. Pu, Analysis of organic Rankine cycles using zeotropic mixtures as working fluids under different restrictive conditions, *Energy Convers. Manage.* 126 (2016) 704–716.
- [10] Y. Zhou, Y. Wu, F. Li, L. Yu, Performance analysis of zeotropic mixtures for the dual-loop system combined with internal combustion engine, *Energy Convers. Manage.* 118 (2016) 406–414.
- [11] J. Li, Y. Duan, Z. Yang, F. Yang, Exergy analysis of novel dual-pressure evaporation organic Rankine cycle using zeotropic mixtures, *Energy Convers. Manage.* 195 (2019) 760–769.
- [12] R. Cipollone, G. Bianchi, M. Di Bartolomeo, D. Di Battista, F. Fatigati, Low grade thermal recovery based on trilateral flash cycles using recent pure fluids and mixtures, *Energy Procedia*. 123 (2017) 289–296.
- [13] Z. Miao, K. Zhang, M. Wang, J. Xu, Thermodynamic selection criteria of zeotropic mixtures for subcritical organic Rankine cycle, *Energy* 167 (2019) 484–497.
- [14] A. Rovira, M. Muñoz, C. Sánchez, R. Barbero, Advanced thermodynamic cycles for finite heat sources: Proposals for closed and open heat sources applications, *Appl. Therm. Eng.* 167 (2020) 114805.
- [15] H. Zhai, Q. An, L. Shi, V. Lemort, S. Quoilin, Categorization and analysis of heat sources for organic Rankine cycle systems, *Renew. Sustain. Energy Rev.* 64 (2016) 790–805.
- [16] W. Su, Y. Hwang, S. Deng, L. Zhao, D. Zhao, Thermodynamic performance comparison of Organic Rankine Cycle between zeotropic mixtures and pure fluids under open heat source, *Energy Convers. Manage.* 165 (2018) 720–737.
- [17] X. Li, J. Song, M. Simpson, K. Wang, P. Sapin, G. Shu, H. Tian, C.N. Markides, Thermo-economic comparison of Organic Rankine and CO₂ cycle systems for low-to-medium temperature applications, in: 5th Int. Semin. ORC Power Syst., Athens, Greece, 2019.
- [18] L. Zhao, J. Bao, The influence of composition shift on organic Rankine cycle (ORC) with zeotropic mixtures, *Energy Convers. Manage.* 83 (2014) 203–211.
- [19] J. Song, C.W. Gu, Analysis of ORC (Organic Rankine Cycle) systems with pure hydrocarbons and mixtures of hydrocarbon and retardant for engine waste heat recovery, *Appl. Therm. Eng.* 89 (2015) 693–702.
- [20] J. Li, Z. Ge, Y. Duan, Z. Yang, Effects of heat source temperature and mixture composition on the combined superiority of dual-pressure evaporation organic Rankine cycle and zeotropic mixtures, *Energy*. 174 (2019) 436–449.
- [21] H. Xi, M.-J.-J. Li, Y.-L.-L. He, Y.-W.-W. Zhang, Economical evaluation and optimization of organic Rankine cycle with mixture working fluids using R245fa as flame retardant, *Appl. Therm. Eng.* 113 (2017) 1056–1070.
- [22] S. Lecompte, B. Ameel, D. Ziviani, M. Van Den Broek, M. De Paepe, Exergy analysis of zeotropic mixtures as working fluids in Organic Rankine Cycles, *Energy Convers. Manage.* 85 (2014) 727–739.
- [23] J. Hærvig, K. Sørensen, T.J. Condra, Guidelines for optimal selection of working fluid for an organic Rankine cycle in relation to waste heat recovery, *Energy*. 96 (2016) 592–602.
- [24] J. Xu, C. Yu, Critical temperature criterion for selection of working fluids for subcritical pressure Organic Rankine cycles, *Energy*. 74 (2014) 719–733.
- [25] Y. Fang, F. Yang, H. Zhang, Comparative analysis and multi-objective optimization of organic Rankine cycle (ORC) using pure working fluids and their zeotropic mixtures for diesel engine waste heat recovery, *Appl. Therm. Eng.* 157 (2019) 113704.
- [26] M.H. Yang, R.H. Yeh, The effects of composition ratios and pressure drops of R245fa/R236fa mixtures on the performance of an organic Rankine cycle system for waste heat recovery, *Energy Convers. Manage.* (2018) 313–326.
- [27] G.S. Chaitanya Prasad, C. Suresh Kumar, S. Srinivasa Murthy, G. Venkatarathnam, Performance of an organic Rankine cycle with multicomponent mixtures, *Energy*. 88 (2015) 690–696.
- [28] M.H. Yang, Payback period investigation of the organic Rankine cycle with mixed working fluids to recover waste heat from the exhaust gas of a large marine diesel engine, *Energy Convers. Manage.* 162 (2018) 189–202.
- [29] F. Heberle, D. Brüggemann, Thermo-economic evaluation of organic Rankine cycles for geothermal power generation using zeotropic mixtures, *Energies*. 8 (2015) 2097–2124.
- [30] Y. Wu, Y. Zhu, L. Yu, Thermal and economic performance analysis of zeotropic mixtures for Organic Rankine Cycles, *Appl. Therm. Eng.* 96 (2016) 57–63.
- [31] B. Dong, G. Xu, T. Li, Y. Quan, J. Wen, Thermodynamic and economic analysis of zeotropic mixtures as working fluids in low temperature organic Rankine cycles, *Appl. Therm. Eng.* 132 (2018) 545–553.
- [32] V.L. Le, A. Kheiri, M. Feidt, S. Pelloux-Prayer, Thermodynamic and economic optimizations of a waste heat to power plant driven by a subcritical ORC (Organic Rankine Cycle) using pure or zeotropic working fluid, *Energy*. 78 (2014) 622–638.
- [33] O.A. Oyewunmi, C.N. Markides, Thermo-economic and heat transfer optimization of working-fluid mixtures in a low-temperature organic Rankine cycle system, *Energies*. 9 (2019) 448.
- [34] Analysis, synthesis, and design of chemical processes, *Choice Rev. Online*. 36 (2013) 36-0974-36-0974.
- [35] S. Mohammadzadeh Bina, S. Jalilinasrabad, H. Fujii, Thermo-economic evaluation of various bottoming ORCs for geothermal power plant, determination of optimum cycle for Sabalan power plant exhaust, *Geothermics*. 70 (2017) 181–191.
- [36] D. Mignard, Correlating the chemical engineering plant cost index with macro-economic indicators, *Chem. Eng. Res. Des.* 92 (2014) 285–294.
- [37] B.K. Saha, B. Chakraborty, P. Pundeer, Thermodynamic and thermo economic analysis of organic Rankine cycle with multi-objective optimization for working fluid selection with low-temperature waste sources in the Indian industry, in: 5th Int. Semin. ORC Power Syst., Athens, Greece, 2019.
- [38] S. Hu, J. Li, F. Yang, Y. Duan, Z. Yang, Thermodynamic, economic and environmental multi-objective optimization of ORC under varying weight, in: 5th Int. Semin. ORC Power Syst., Athens, Greece, 2019.
- [39] J. Li, Y. Duan, Z. Yang, Thermo-economic analysis of dual-pressure evaporation Organic Rankine Cycle system using R245fa, in: 5th Int. Semin. ORC Power Syst., Athens, Greece, 2019.
- [40] Z. Shengjun, W. Huaixin, G. Tao, Performance comparison and parametric optimization of subcritical Organic Rankine Cycle (ORC) and transcritical power cycle system for low-temperature geothermal power generation, *Appl. Energy*. 88 (2011) 2740–2754.
- [41] A.I. Papadopoulos, M. Stijepovic, P. Linke, On the systematic design and selection of optimal working fluids for Organic Rankine Cycles, *Appl. Therm. Eng.* 30 (2010) 760–769.
- [42] M.H. Yang, R.H. Yeh, T.C. Hung, Thermo-economic analysis of the transcritical organic Rankine cycle using R1234yf/R32 mixtures as the working fluids for lower-grade waste heat recovery, *Energy*. 140 (2017) 818–836.
- [43] M.H. Yang, Optimizations of the waste heat recovery system for a large marine diesel engine based on transcritical Rankine cycle, *Energy*. 113 (2016) 1109–1124.
- [44] H. Tian, L. Chang, Y. Gao, G. Shu, M. Zhao, N. Yan, Thermo-economic analysis of zeotropic mixtures based on siloxanes for engine waste heat recovery using a dual-loop organic Rankine cycle (DORC), *Energy Convers. Manage.* 136 (2017) 11–26.
- [45] F. Heberle, D. Brüggemann, Thermo-economic analysis of zeotropic mixtures and pure working fluids in Organic Rankine Cycles for waste heat recovery, *Energies*. 9 (2016).
- [46] D. Kern, *Process Heat Transfer*, McGraw-Hill, New York, 1950.
- [47] V. Gnielinski, *New Equations for Heat and Mass Transfer in Turbulent Pipe and Channel Flow*, *Int. Chem. Eng.*, 1976.
- [48] K.E. Gungor, R.H.S. Winterton, Simplified general correlation for saturated flow boiling and comparisons of correlations with data, *Chem. Eng. Res. Des.* (1987).
- [49] J.R. Thome, Prediction of the mixture effect on boiling in vertical thermosiphon reboilers, *Heat Transf. Eng.* (1989).
- [50] M.M. Shah, An improved and extended general correlation for heat transfer during condensation in plain tubes, *HVAC R Res.* 15 (2009) 889–913.
- [51] K.K.J. Bell, M.A. Ghaly, Approximate generalized design method for multi-component/partial condensers, in: *AIChE Pap.*, 1972.
- [52] J. Radulovic, N.I. Beleno Castaneda, On the potential of zeotropic mixtures in supercritical ORC powered by geothermal energy source, *Energy Convers. Manage.* 88 (2014) 365–371.
- [53] Z. Miao, X. Yang, J. Xu, J. Zou, Development and dynamic characteristics of an Organic Rankine Cycle, *Chinese Sci. Bull.* 59 (2014) 4367–4378.
- [54] D. Maraver, J. Royo, V. Lemort, S. Quoilin, Systematic optimization of subcritical and transcritical organic Rankine cycles (ORCs) constrained by technical parameters in multiple applications, *Appl. Energy*. 117 (2014) 11–29.
- [55] H. Zhai, Q. An, L. Shi, Analysis of the quantitative correlation between the heat source temperature and the critical temperature of the optimal pure working fluid for subcritical organic Rankine cycles, *Appl. Therm. Eng.* 99 (2016) 383–391.
- [56] Y.R. Li, M.T. Du, C.M. Wu, S.Y. Wu, C. Liu, Potential of organic Rankine cycle using zeotropic mixtures as working fluids for waste heat recovery, *Energy*. 77 (2014) 509–519.
- [57] J. Vivian, G. Manente, A. Lazzaretto, A general framework to select working fluid and configuration of ORCs for low-to-medium temperature heat sources, *Appl. Energy*. 156 (2015) 727–746.
- [58] M. Chys, M. van den Broek, B. Vanslambrouck, M. De Paepe, Potential of zeotropic mixtures as working fluids in organic Rankine cycles, *Energy*. 44 (2012) 623–632.